J|A|C|S
ARTICLES
Published on Web 07/17/2002

Theoretical Study on Second Hyperpolarizabilities of Phenylacetylene Dendrimer: Toward an Understanding of Structure−Property Relation in NLO Responses of Fractal Antenna Dendrimers

Masayoshi Nakano,* Harunori Fujita, Masahiro Takahata, and Kizashi Yamaguchi

Contribution from the Department of Chemistry, Graduate School of Science, Osaka University, Toyonaka, Osaka 560-0043, Japan

Received June 28, 2001. Revised Manuscript Received March 22, 2002

Abstract: This contribution explores the relation between molecular second hyperpolarizabilities (γ) and molecular architecture in phenylacetylene dendrimers using the semiempirical molecular orbital method, that is, INDO/S method. The orientationally averaged γ of a large-size phenylacetylene dendrimer, which is composed of 24 units of phenylacetylenes and is referred to as D25, is found to be about 50 times as large as that of the diphenylacetylene monomer. In contrast, the γ_s value of D25 is found to be about 6 times as small as that of the *para*-substituted phenylacetylene oligomer (L25) composed of 24 units of phenylacetylenes. To investigate the structure−property relation in γ for D25 and L25, we examine the spatial contributions of electrons to γ values using γ density analysis. The present analysis reveals that the dominant contributions of electrons to γ of D25 are localized in the linear-leg regions parallel to the applied electric field and the contributions are also well segmented at the *meta*-connected points (benzene rings), while the spatial distribution of the γ density of L25 is extended over the whole region of the chain, and the dominant contribution stems from the both-end regions. It is found for D25 that the magnitude of contributions to γ in the internal region is more enhanced than that in the outer region. We further found that the magnitudes of contributions in internal linear-leg regions of D25 are somewhat larger than those of the same-size isolated linear-leg molecules. This suggests that the slightly remaining π-conjugations via the *meta*-branching points still enhance the contributions to γ localized in the linear-leg regions. These features of spatial contributions to γ of D25 are found to originate in the fractal architecture, in which π-conjugation lengths in the linear-leg region increase on going from the periphery to the core. Finally, fractal antenna dendrimers are expected to be promising novel nonlinear optical (NLO) substances with a controllability of the magnitude and spatial contribution of the third-order NLO properties.

Introduction

For the past two decades, organic molecular systems that exhibit large nonlinear optical (NLO) responses have attracted great attention in scientific and technological fields because of their large susceptibilities, fast responsibility, and possibility of modification.[1−4] The organic NLO effects originate in the microscopic nonlinear polarization mainly enhanced by π-electron conjugation at the molecular level. Such microscopic nonlinear polarization is characterized by the hyperpolarizabilities. A variety of organic π-conjugated molecular systems, for example, donor−acceptor substituted polymeric systems, polyaromatic systems, and molecular crystal systems composed of donor and acceptor molecules, have been intensely investigated by virtue of their low-excitation energies and large transition properties.

Recently, a new class of polymeric systems, that is, dendrimers, is of considerable interest because of its high controllability of architecture and its high light-harvesting property.[5−14] In general, dendrimers are characterized by a large number of

* To whom correspondence should be addressed. E-mail: mnaka@chem.sci.osaka-u.ac.jp.

(1) Williams, D. J., Ed. *Nonlinear Optical Properties of Organic and Polymeric Materials*; ACS Symposium Series 233; American Chemical Society: Washington, DC, 1984.
(2) Prasad, N. P.; Williams, D. J. *Introduction to Nonlinear Optical Effects in Molecules and Polymers*; Wiley: New York, 1991.
(3) (a) Kanis, D. R.; Ratner, M. A.; Marks, T. J. *Chem. Rev.* **1994**, *94*, 195. (b) Brédas, J. L.; Adant, C.; Tackx, P.; Persoons, A. *Chem. Rev.* **1994**, *94*, 243.
(4) (a) Nakano, M.; Yamaguchi, K. Analysis of Nonlinear Optical Processes for Molecular Systems. *Trends in Chemical Physics*; Research Trends: Trivandrum, India, 1997; Vol. 5, pp 87−237. (b) Nakano, M.; Okumura, M.; Yamaguchi, K.; Fueno, T. *Mol. Cryst. Liq. Cryst.* **1990**, *182A*, 1. (c) Nakano, M.; Yamaguchi, K. *Chem. Phys. Lett.* **1993**, *206*, 285.
(5) Knox, R. S. In *Primary Processes of Photosynthesis*; Barber, J., Ed.; Elsevier: Amsterdam, 1977; p 55.
(6) Pope, M.; Swenberg, C. E. *Electronic Processes in Organic Crystals*; Oxford University Press: Oxford, 1982.
(7) Tomalia, D. A.; Baker, H.; Dewald, J. R.; Hall, M.; Kallos, G.; Martin, S.; Roeck, J.; Ryder, J.; Smith, *P. Polym. J.* **1985**, *17*, 117.
(8) Webber, S. E. *Chem. Rev.* **1990**, *90*, 1469.
(9) Tomalia, D. A.; Naylor, A. M.; Goddard, W. A. *Angew. Chem., Int. Ed. Engl.* **1990**, *29*, 138.
(10) Hawker, C.; Fréchet, J. M. J. *J. Am. Chem. Soc.* **1990**, *112*, 7638.
(11) Fox, M. A.; Jones, W. E.; Watkins, D. M. *Chem. Eng. News* **1993**, *119*, 6197.
(12) Fréchet, J. M. J. *Science* **1994**, *263*, 1710.
(13) Adronov, A.; Fréchet, J. M. J. *Chem. Commun.* **2000**, 1701
(14) Grayson, S. K.; Fréchet, J. M. J. *Chem. Rev.* **2001**, *101*, 3819.

10.1021/ja0115969 CCC: $22.00

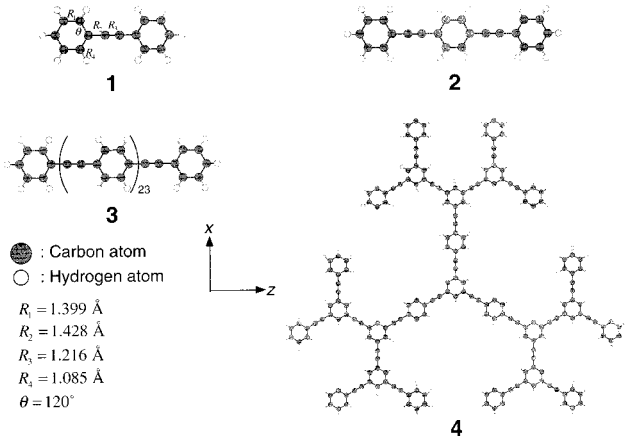

Figure 1. Structures of diphenylacetylene **1**, bis(phenylacetylene)-benzene **2**, *para*-substituted phenylacetylene oligomer (L25) **3**, and phenylacetylene dendrimer (D25) **4** with a planar fractal antenna structure made of 24 units of phenylacetylenes. The bond lengths ($R_1 = 1.399$ Å, $R_2 = 1.428$ Å, $R_3 = 1.216$ Å, and $R_4 = 1.085$ Å) and bond angles ($\theta = 120°$) of diphenylacetylene (partially optimized by the B3LYP method using 6-31G** basis sets) are used for these systems.

terminal groups originating in a focal point (core) with at least one branch at each repeat unit. Particularly, the Cayley-tree-type dendrimers with fractal antenna structures composed of phenyl rings and acetylene units, which are referred to as phenylacetylene dendrimers (see Figure 1, compound **4**), have actually been synthesized and exhibit efficient energy migration from the periphery to the core.[15−19] In these molecules, the "fractal structure" means that the lengths of linear-leg regions involved in the dendritic structure increase on going from the periphery to the core. The efficient excitation energy cascades to the core is assumed to be caused by the facts that the molecular architecture provides an exciton funnel with a well-directed energy gradient as the energy decreases as a function of position from the periphery to the core and that the exciton−phonon coupling causes the relaxation among the exciton states.[20] In our previous papers,[21,22] therefore, we elucidated the features of exciton states and exciton migration dynamics of some dendritic molecular aggregates modeled after phenylacetylene dendrimers. However, there have been a few studies on other electronic functionalities, for example, (non)linear optical response properties, for such systems except for the first-order optical processes, that is, absorption and emission of light.

For phenylacetylene dendrimers, π-conjugation in their linear-leg (*para*-substituted phenylacetylene) regions and its decoupling at the *meta*-connected points (benzene rings) are predicted to be important to generate multistep energy structures and efficient exciton migration from the periphery to the core.[15−19] Such unique features of π-conjugation in fractal structures are also expected to provide a remarkable influence on the NLO response properties because the π-conjugation is known to sensitively affect the NLO properties for such systems. In fact, the size-dependencies of NLO properties of phenylene vinylene oligomers, modeled after linear-leg regions connected with *meta*-substituted benzene rings, were shown to sensitively reflect the change in the length of π-conjugation (well localized in linear-leg region), which gradually increases on going from one end to the other end in the chain-length direction. This suggests that the fractal feature in the π-conjugation length in fractal antenna dendrimers is closely related to the size-dependencies of NLO properties.[23] However, the actual Cayley-tree-type phenylacetylene dendrimers have a fractal dimension D ($1 < D < 2$), so that the structure−property relation in γ for such dendrimers should be considered on the basis of orientationally averaged values, γ_s, involving several components of γ_{ijkl}.

In this study, therefore, we report the first theoretical study on γ_s of the entire system of a phenylacetylene dendrimer composed of 24 phenylacetylene units, which is referred to as D25 hereafter (see Figure 1, compound **4**), using a simple semiempirical molecular orbital (MO) method treating all valence electrons, that is, INDO/S method.[24] To ensure the reliability of this method, we compare the INDO/S results for longitudinal γ values of diphenylacetylene and bis(phenylacetylene)-benzene with those by ab initio Hartree−Fock (HF), Møller−Plesset second-order perturbation (MP2), and hybrid density functional (DF), that is, B3LYP,[25,26] methods with standard and extended basis sets. As a reference to D25, we also examine the γ values and γ density of a *para*-substituted phenylacetylene oligomer (L25) involving the same number of benzene rings (25).

The finite-field (FF) approach[27] using the INDO/S coupled Hartree−Fock (CHF)[28] method is applied to the evaluation of several components of γ_{ijkl} required to obtain a γ_s value of D25 and L25. To pictorially elucidate the structure−property relation in γ of these systems, we perform the γ density analysis[29,30] (using third-order derivatives of charge densities with respect to applied electric fields), which can visualize the contributions of electrons in arbitrary spatial regions to γ. The relations among the fractal architecture, the γ value, and the spatial contributions of electrons to γ are explored and then are discussed in relation to the possibility of designing novel third-order NLO materials with desired magnitude and spatial contributions to γ.

Calculational Details

Second Hyperpolarizability. Because the macroscopic optical polarization of molecular-based materials is described by the microscopic response of the constituent molecules, the molecular optical response can be described in a power series expansion of the molecular polarization p^i (the i component of polarization oscillating at angular frequency ω) by an external electric field:

$$p^i(\omega) = \sum_j \alpha_{ij} F^j(\omega_1) + \sum_{jk} \beta_{ijk} F^j(\omega_1) F^k(\omega_2) + \sum_{jkl} \gamma_{ijkl} F^j(\omega_1) F^k(\omega_2) F^l(\omega_3) + ... \quad (1)$$

(15) Devadoss, C.; Bharathi, P.; Moore, J. S. *J. Am. Chem. Soc.* **1996**, *118*, 9635.
(16) Shortreed, M. R.; Swallen, S. F.; Shi, Z.-Y.; Tan, W.; Xu, Z.; Devadoss, C.; Moore, J. S.; Kopelman, R. *J. Phys. Chem. B* **1997**, *101*, 6318.
(17) Kopelman, R.; Shortreed, M.; Shi, Z.-Y.; Tan, W.; Bar-Haim, A.; Klafter, J. *Phys. Rev. Lett.* **1997**, *78*, 1239.
(18) Bar-Haim, A.; Klafter, J.; Kopelman, R. *J. Am. Chem. Soc.* **1997**, *119*, 6197.
(19) Tretiak, S.; Chernyak, V.; Mukamel, S. *J. Phys. Chem. B* **1998**, *102*, 3310.
(20) (a) Harigaya, H. *Int. J. Mod. Phys. B* **1999**, *13*, 2531. (b) Harigaya, H. *Phys. Chem. Chem. Phys.* **1999**, *1*, 1687.
(21) Nakano, M.; Takahata, M.; Fujita, H.; Kiribayashi, S.; Yamaguchi, K. *Chem. Phys. Lett.* **2000**, *323*, 249.
(22) (a) Takahata, M.; Fujita, H.; Nakano, M.; Kiribayashi, S.; Nagao, H.; Yamaguchi, K. *Nonlinear Opt.* **2000**, *26*, 177. (b) Fujita, H.; Takahata, M.; Nakano, M.; Kiribayashi, S.; Nagao, H.; Yamaguchi, K. *Nonlinear Opt.* **2000**, *26*, 185.
(23) Nakano, M.; Fujita, H.; Takahata, M.; Yamaguchi, K. *J. Chem. Phys.* **2001**, *115*, 1052. (b) Nakano, M.; Fujita, H.; Takahata, M.; Yamaguchi, K. *J. Chem. Phys.* **2001**, *115*, 6780.
(24) Ridley, J.; Zerner, M. C. *Theor. Chim. Acta* **1973**, *32*, 111; **1976**, *42*, 223; **1979**, *53*, 21.

Here, $F^i(\omega_1)$ represents the i component of the applied electric field oscillating at ω_1. α_{ij}, β_{ijk}, and γ_{ijkl} are the tensor components of the polarizability, the first hyperpolarizability, and the second hyperpolarizability, respectively. γ is responsible for the third-order NLO phenomena, for example, third-harmonic generation (THG), and is the quantity of interest in this study. Although the frequency dependence of hyperpolarizabilities in eq 1 is important in the case of near-resonant nonlinear optical phenomena, we focus on the off-resonant third-order nonlinear optical phenomena in this study, where the static γ is considered to be a good approximation to the off-resonant frequency dependent γ. In experiments of THG, the macroscopic third-order nonlinear optical susceptibility is related to the orientationally averaged second hyperpolarizability, γ_s, which is expressed (in the static case) by[1−4]

$$\gamma_s = \frac{1}{5}(\gamma_{xxxx} + \gamma_{yyyy} + \gamma_{zzzz} + 2\gamma_{xxyy} + 2\gamma_{yyzz} + 2\gamma_{zzxx}) \quad (2)$$

Finite-Field Calculation. Various theoretical approaches for calculating γ have been presented in the literature. The sum-over-state (SOS) approach[1−4] based on the time-dependent perturbation theory (TDPT) is useful for elucidating the contribution of transitions between electronic excited states to γ. Alternatively, the approaches using numerical or analytical derivatives of total energy with respect to the applied electric field are widely employed for calculating static γ. Particularly, the FF approach using the CHF method at the semiempirical[31] and ab initio[32] MO levels, various electron-correlated ab initio MO methods,[33] and the DF methods[34−37] has been widely employed for calculating static (hyper)polarizabilities. Because the excessively large size of the target molecule such as D25 prohibits applying most of the ab initio MO and DF methods using extended basis sets to the calculation of γ, the semiempirical MO methods will be appropriate for the qualitative or semiquantitative description of γ for such large-size systems.[31] We here employ the INDO/S method to obtain the total energies of a molecule under the applied electric fields.

Static γ_{ijkl} ($i, j, k, l = x, y, z$) is obtained by the fourth derivative of total energy E with respect to the applied field. Because the phenylacetylene dendrimer has a planar architecture, we should consider the averaged γ_s in eq 2, which includes two types of components of γ, that is, γ_{iiii} and γ_{iijj}. These γ values are calculated by the numerical differentiation of the total energy E with respect to the applied electric field:

$$\gamma_{iiii} = \{E(3F^i) - 12E(2F^i) + 39E(F^i) - 56E(0) + 39E(-F^i) - 12E(-2F^i) + E(-3F^i)\}/\{36(F^i)^4\} \quad (3)$$

and

$$\gamma_{iijj} = -\{E(F^i,F^j) + E(-F^i,F^j) + E(F^i,-F^j) + E(-F^i,-F^j) - 2[E(F^j) + E(-F^j) + E(F^i) + E(-F^i)] + 4E(0)\}/\{6(F^i)^4\} \quad (4)$$

where $E(F^i)$ represents the total energy in the presence of the electric field F applied in the i direction. This method is referred to as the FF method. To avoid numerical errors, we use several minimum field strengths. After numerical differentiations using these fields (0.0002−0.001 au), we adopt numerically stable γ values for various π-conjugated systems considered in this study.

Hyperpolarizability Density Analysis. The hyperpolarizability density analysis method provides the spatial contributions of electrons to hyperpolarizabilities.[29,30] Such spatial contributions of electrons to hyperpolarizabilities provide a local view of hyperpolarizability although it is generally a global value. This is expected to be useful for chemists to intuitively and pictorially understand the mechanism of hyperpolarizabilities and to construct the design rule of nonlinear optical molecules. Although the analysis method can be extended to treat the dynamic (frequency-dependent) hyperpolarizabilities and to divide the spatial contributions to each virtual excitation process,[38] we here briefly explain the static hyperpolarizability density analysis in the FF approach for the following discussion.

Before explaining our density analysis, it is worthwhile to mention another real-space analysis of hyperpolarizabilities developed by Mukamel's group.[39,40] Their method is based on the plots of kth-order contribution of time-dependent density matrix in external fields and has the advantage of elucidating the contribution of off-diagonal density (which represents the size of exciton radius (coherence size)) in addition to the diagonal (charge) density. Although our analysis using dynamic hyperpolarizability density[38] is similar to their method, in our analysis the off-diagonal density disappears, and a quantity like a charge density (hyperpolarizability density) is treated. The effect of off-diagonal density is considered to be reflected in the feature of hyperpolarizability density distribution. Because the hyperpolarizability density is also simply connected to hyperpolarizability as shown below (eq 5), we use our density analysis in this study.

From the expansion formula of charge density in powers of the electric field and eq 1, the second hyperpolarizability can be expressed by

$$\gamma_{ijkl} = -\frac{1}{3!}\int r^i \rho^{(3)}_{jkl}(\mathbf{r}) d^3\mathbf{r} \quad (5)$$

where

$$\rho^{(3)}_{jkl}(\mathbf{r}) = \frac{\partial^3 \rho}{\partial F^j \partial F^k \partial F^l}\Big|_{F=0} \quad (6)$$

Here, r^i is the i component of the electron coordinate. This third derivative $\rho^{(3)}_{jkl}(\mathbf{r})$ of electron density with respect to external electric fields is referred to as the second hyperpolarizability (γ) density. Other (hyper)polarizability densities are also defined in a similar manner.[30] This quantity can be calculated in a good precision by discretizing the space and by using the efficient numerical differentiation method. The numerically precise value of this density is useful for investigating the effects of basis sets and electron correlations on the hyperpolarizabilities of three-dimensional systems in the ab initio MO method.[4,36,37]

Because we here evaluate the characteristics of γ of large-size molecules using the semiempirical MO method, the γ density analysis is performed approximately using the Mulliken charge densities. Such approximate γ density analysis using the Mulliken charge density has

(25) (a) Becke, A. D. *Phys. Rev. A* **1988**, *38*, 3098. (b) Becke, A. D. *Int. J. Quantum Chem. Symp.* **1989**, *23*, 599. (c) Becke, A. D. *J. Chem. Phys.* **1993**, *98*, 5648.
(26) Lee, C.; Yang, W.; Parr, R. G. *Phys. Rev.* **1988**, *37*, 786.
(27) Cohen, H. D.; Roothaan, C. C. J. *J. Chem. Phys.* **1965**, *S34*, 43.
(28) Karna, S. P.; Prasad, S. P.; Dupuis, M. *J. Chem. Phys.* **1991**, *94*, 1171.
(29) Nakano, M.; Yamaguchi, K.; Fueno, T. *Chem. Phys. Lett.* **1991**, *185*, 550.
(30) Nakano, M.; Shigemoto, I.; Yamada, S.; Yamaguchi, K. *J. Chem. Phys.* **1995**, *103*, 4175.
(31) (a) Kirtman, B.; Hasan, M. *Chem. Phys. Lett.* **1989**, *157*, 123. (b) Kanis, D. R.; Ratner, M. A.; Marks, T. J. *J. Am. Chem. Soc.* **1990**, *112*, 8203. (c) Kanis, D. R.; Ratner, M. A.; Marks, T. J.; Zerner, M. C. *Chem. Mater.* **1991**, *3*, 19. (d) Kanis, D. R.; Ratner, M. A.; Marks, T. J. *J. Am. Chem. Soc.* **1992**, *114*, 10338. (e) Kanis, D. R.; Ratner, M. A.; Marks, T. J. *Int. J. Quantum Chem.* **1992**, *43*, 61.
(32) Hurst, G. J.; Dupuis, M. *Chem. Phys. Lett.* **1990**, *171*, 201.
(33) (a) Sekino, H.; Bartlett, R. *J. Chem. Phys.* **1991**, *94*, 3665. (b) Kobayashi, T.; Sasagane, K.; Aiga, F.; Yamaguchi, K. *J. Chem. Phys.* **1999**, *110*, 11720. (c) Larsen, H.; Olsen, J.; Hättig, C.; Jørgensen, P.; Christiansen, O.; Gauss, J. *J. Chem. Phys.* **1999**, *111*, 1917.
(34) Matsuzawa, N.; Dixon, D. A. *J. Phys. Chem.* **1994**, *98*, 2545.
(35) Calaminici, P.; Jug, K.; Köester, A. M. *J. Chem. Phys.* **1998**, *109*, 7756.
(36) Yamada, S.; Nakano, M.; Shigemoto, I.; Yamaguchi, K. *Chem. Phys. Lett.* **1996**, *254*, 158.
(37) Yamada, S.; Nakano, M.; Yamaguchi, K. *J. Phys. Chem.* **1999**, *103*, 7105.
(38) (a) Nakano, M.; Yamada, S.; Shigemoto, I.; Yamaguchi, K. *Chem. Phys. Lett.* **1996**, *250*, 247. (b) Nakano, M.; Fujita, H.; Takahata, M.; Yamaguchi, K. *Chem. Phys. Lett.* **2002**, *356*, 462. (c) Fujita, H.; Nakano, M.; Takahata, M.; Yamaguchi, K. *Chem. Phys. Lett.* **2002**, *358*, 435.
(39) Wagersreiter, T.; Mukamel, S. *J. Chem. Phys.* **1996**, *104*, 7086.
(40) Schulz, M.; Tretiak, S.; Chernyak, V.; Mukamel, S. *J. Am. Chem. Soc.* **2000**, *122*, 452.

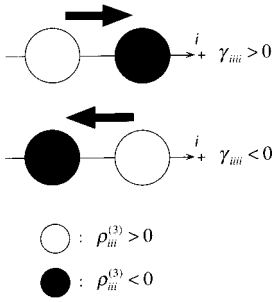

Figure 2. Schematic diagram of the second hyperpolarizability (γ_{iiii}) densities $\rho^{(3)}_{iii}(\mathbf{r})$. The white and black circles represent the positive and negative $\rho^{(3)}_{iii}(\mathbf{r})$, respectively. The size of the circle represents the magnitude of $\rho^{(3)}_{iii}(\mathbf{r})$, and the arrow shows the sign of γ_{iiii} determined by the relative spatial configuration between these two $\rho^{(3)}_{iii}(\mathbf{r})$.

been shown to be useful.[29,30,41−44] The approximate γ_{ijkl} is represented by

$$\gamma_{ijkl} \cong -\frac{1}{3!}\sum_s r^i_s \rho^{\mathrm{app}\,(3)}_{ss,jkl} \tag{7}$$

where

$$\rho^{\mathrm{app}\,(3)}_{ss,jkl} = \frac{\partial^3 \rho^{\mathrm{app}}_{ss,jkl}}{\partial F^j \partial F^k \partial F^l}\Big|_{F=0} \tag{8}$$

This quantity represents the γ density in the Mulliken approximation. Here, r^i_s represents the i component of the coordinate of the atom located at the center of the atomic orbital s. The quantity $\rho^{\mathrm{app}\,(3)}_{ss,iii}$, which is the γ_{iiii} density of atomic orbital s, is calculated by the four-point numerical differentiation method as follows.

$$\rho^{\mathrm{app}\,(3)}_{ss,iii} = \{\rho^{\mathrm{app}}_{ss,iii}(2F^i) - \rho^{\mathrm{app}}_{ss,iii}(-2F^i) - 2(\rho^{\mathrm{app}}_{ss,iii}(F^i) - \rho^{\mathrm{app}}_{ss,iii}(-F^i))\}/\{2(F^i)^3\} \tag{9}$$

where $\rho^{\mathrm{app}}_{ss,iii}(F^i)$ is the Mulliken charge density of the atomic orbital s in the presence of the electric field F^i. Other approximate (hyper)-polarizability densities can be also calculated using the numerical differentiation method.[30]

To explain a method for analysis employing the plots of γ densities, we consider a pair of localized $\rho^{(3)}_{iii}(\mathbf{r})$ shown in Figure 2. The positive sign of $\rho^{(3)}_{iii}(\mathbf{r})$ implies that the second derivative of the charge density increases with the increase in the field. As can be seen from eqs 5 and 7, the arrow from positive to negative $\rho^{(3)}_{iii}(\mathbf{r})$ shows the sign of the contribution to γ_{iiii} determined by the relative spatial configuration between the two $\rho^{(3)}_{iii}(\mathbf{r})$. The sign of the contribution to γ_{iiii} becomes positive when the direction of the thick arrow coincides with the positive direction of the coordinate system. The contribution to γ_{iiii} determined by $\rho^{(3)}_{iii}(\mathbf{r})$ of the two points is more significant when their distance is larger.

Phenylacetylene-Based Systems. Figure 1 shows the geometries of diphenylacetylene **1**, bis(phenylacetylene)-benzene **2**, *para*-substituted phenylacetylene oligomer (L25) **3**, and phenylacetylene dendrimer (D25) **4** with a planar fractal antenna structure on the $z-x$ plane. D25 is constructed from linear-leg regions involving *para*-connected phenylacetylenes and the *meta*-connected benzene rings. Central generation involves longer linear-leg regions as compared to the outer region. Such dendrimers have a fractal structure in a sense that the lengths of the linear-leg regions increase on going from the periphery to the core. Because we focus on the qualitative structure−property relation of γ for these systems, we use the bond lengths ($R_1 = 1.399$ Å, $R_2 = 1.428$ Å, $R_3 = 1.216$ Å, and $R_4 = 1.085$ Å) and bond angles ($\theta = 120°$) of diphenylacetylene (partially optimized by the B3LYP method using 6-31G** basis sets) for these systems. The B3LYP method is known to well reproduce the experimental geometries of organic molecular systems.[34,35] In this study, the B3LYP calculation is performed using the Gaussian 94 package.[45]

Results and Discussion

Comaprison of Longitudinal γ Values of Diphenylacetylene and Bis(phenylacetylene)-benzene Calculated by Several Ab Initio, Density Functional, and INDO/S Methods. As mentioned above, the CHF method in the INDO/S approximation is known to provide qualitatively or semiquantitatively well results of γ for large-size organic molecules. However, to check the reliability of our calculations using the INDO/S method, we examine the longitudinal γ values, γ_{zzzz} (which is a dominant component of γ), of diphenylacetylene (compound **1**) and bis-(phenylacetylene)-benzene (compund **2**) by comparing the INDO/S CHF results with several ab initio and density functional, that is, B3LYP, results. Although previous studies on the γ values and their densities of relatively small-size organic systems[4,34−37] show that the B3LYP method using extended basis sets can well reproduce those values calculated by the ab initio methods including high-order electron correlations, the longitudinal γ values and their size-dependencies for large-size π-conjugated molecules calculated by the B3LYP method are found to be overestimated as compared to the results of the ab initio methods including sufficient electron correlation effects.[46] Therefore, we apply the HF and Møller−Plesset second-order perturbation (MP2) methods, which are known to efficiently include electron-correlation effects for these types of compounds, in addition to the B3LYP methods. Also, to check the effects of basis sets, we use the standard basis set, 6-31G**, and an extended basis set, 6-31G**+d ($\zeta_d = 0.0523$ on carbon atoms), which is widely used for the calculation of the γ of π-conjugated organic molecules.[4,32]

The size-dependencies of γ per diphenylacetylene unit (γ/n) of compounds **1** and **2** calculated by these methods are shown in Figure 3. It is found from the comparison of results using the 6-31G** basis set with those using the 6-31G**+d basis set at the HF and B3LYP levels that the augmentation of diffuse d function hardly changes the increasing rate of γ/n as the number of units increases and just slightly enhances the magnitudes of γ/n (16% enhanced for compound **2** at the HF level). This feature agrees well with the previous result that the effects of diffuse function on the longitudinal components of γ/n become small as the π-conjugation lengths of linear-chain molecules increase.[32] The electron correlation effects at the MP2/6-31G** level are found to enhance the magnitudes (54% enhanced for compound **2**) and slightly increase the rate of γ/n

(41) An, Z.; Wong, K. Y. *J. Chem. Phys.* **2001**, *114*, 1010.
(42) Jacquemin, D.; Beljonne, D.; Champagne, B.; Geskin, V.; Brédas, J.-L.; André, J.-M. *J. Chem. Phys.* **2001**, *115*, 6766.
(43) Bishop, D. M.; Bouferguene, A. *Int. J. Quantum Chem.* **2000**, *78*, 348.
(44) Brédas, J.-L.; Adant, C.; Tackx, P.; Persoons, A. *Chem. Rev.* **1994**, *94*, 243.
(45) Frisch, M. J.; Trucks, G. W.; Head-Gordon, M.; Gill, P. M. W.; Wong, M. W.; Foresman, J. B.; Johnson, B. G.; Schlegel, H. B.; Robb, M. A.; Replogle, E. S.; Gomperts, R.; Andres, J. L.; Raghavachari, K.; Binkley, J. S.; Gonzalez, C.; Martin, R. L.; Fox, D. J.; Defrees, D. J.; Baker, J.; Stewart, J. J. P.; Pople, J. A. *Gaussian 94*, revision B.1; Gaussian, Inc.: Pittsburgh, PA, 1995.
(46) (a) van Gisbergen, S. J. A.; Schipper, P. R. T.; Gritsenko, O. V.; Baerends, E. J.; Snijders, J. G.; Champagne, B.; Kirtman, B. *Phys. Rev. Lett.* **1999**, *84*, 694. (b) Champagne, B.; Perpéte, E. A.; van Gisbergen, S. J. A.; Baerends, E.; Snijders, J. G.; Soubra-Ghaoui, C.; Robins, K. A.; Kirtman, B. *J. Chem. Phys.* **1999**, *108*, 10489.

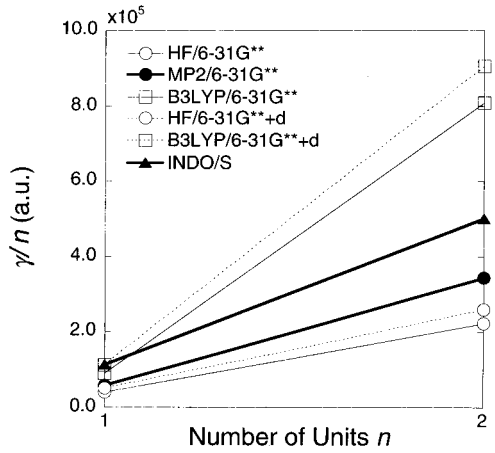

Figure 3. Size-dependencies of longitudinal γ per diphenylacetylene unit (γ/n) of compounds **1** and **2** (see Figure 1) calculated by the HF, MP2, B3LYP, and INDO/S methods. Two types of basis sets, a standard (6-31G**) and an extended (6-31G**+d) ($\zeta_d = 0.0523$ on carbon atoms) basis set, are used except for the MP2 and INDO/S methods.

(a) Compound **1** γ= 113100 a.u. (INDO/S)

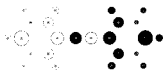

(b) Compound **2** γ= 501400 a.u. (INDO/S)

Figure 4. Longitudinal component values, γ_{zzzz}, and their density plots (in the Mulliken approximation) of diphenylacetylene **1** and bis(phenylacetylene)-benzene **2** (see Figure 1) calculated by the INDO/S method. Lighter areas represent the spatial regions with larger γ_{zzzz} densities.

at the HF/6-31G** level. The increasing rate of γ/n at the INDO/S level is shown to be similar to that at the MP2/6-31G** level although the magnitudes of γ/n values at the INDO/S level are larger than those at the MP2/6-31G** level (46% enhanced for compound **2**). In contrast, the B3LYP results using the 6-31G** and 6-31G**+d basis sets apparently remarkably overestimate both the magnitude and the increasing rate of γ/n by other methods; the γ/n for compound **1** at the B3LYP/6-31G** level is 240% enhanced as compared to that at the MP2/6-31G** level. This feature coincides with the fact observed by van Gisbergen and collaborators.[46] The B3LYP method is shown to be insufficient for reproducing the correct tendency of the magnitude and size-dependency of γ/n for large-size π-conjugated molecules. Judging from these results, we expect that the qualitative γ values for phenylacetylene oligomers can be reproduced by the INDO/S CHF calculations. Therefore, we use the INDO/S results for the following discussion.

Figure 4 shows the γ densities, $\rho^{(3)}_{zzz}(\boldsymbol{r})$, for compounds **1** and **2** at the INDO/S level. The γ densities are drawn at the plane located at 1 au (~0.52917 Å) above the molecular plane to mainly examine the contribution of π-electrons. It is found from Figure 4a that the main contribution originates in the positive contribution from benzene-ring regions, while the acetylene region gives only a slight negative contribution. This feature suggests that π-conjugation effects between benzene rings provide positive contributions to γ. For compound **2** (Figure 4b), both-end phenylacetylenes provide a main contribution with a large positive value, while the central benzene-ring region provides a small negative contribution. This feature suggests that the π-conjugation effect over both-end benzene-ring regions determines the γ value of compound **2**.

Table 1. γ_{xxxx}, γ_{yyyy}, γ_{zzzz}, γ_{xxyy}, γ_{yyzz}, γ_{zzxx}, and the Orientationally Averaged γ (γ_s) Values [au] (eq 2) of L25 and D25 Shown in Figure 1

components	L25	D25
γ_{xxxx}	19 560	2 171 000
γ_{yyyy}	12 230	567.5
γ_{zzzz}	27 330 000	2 170 000
γ_{xxyy}	8 076	13 430
γ_{yyzz}	463 800	13 370
γ_{zzxx}	4 099 000	72 800
γ_s	7 302 000	1 170 000

γ and γ Densities of L25 and D25. We investigate several components of γ_{ijkl} and their densities of D25. To clarify the structure dependence of γ, we also examine the γ values and γ density of a linear-chain oligomer involving the same number of benzene rings (25), that is, *para*-substituted phenylacetylene oligomer (L25) (see Figure 1, compound **3**). Each component of the calculated γ_{ijkl} values in eq 2 and the averaged values, γ_s, for L25 and D25 are given in Table 1. As expected from their structures, the γ_s of L25 is dominantly determined by the longitudinal component, that is, γ_{zzzz} (=27 330 000 au), for L25, while the γ_s of D25 is done by the two components, that is, γ_{xxxx} (=2 171 000 au) and γ_{zzzz} (=2 170 000 au). For comparison, we also examine the interaction unit monomer, that is, diphenylacetylene (see Figure 1, compound **1**), the γ_s (=23 250 au) of which is dominantly determined by the longitudinal component. It is found that the total γ_s of L25 (7 302 000 au) is found to be about 6 times as large as that of D25 (1 170 000 au), which is about 50 times as large as that of monomer (diphenylacetylene). Because the present dendrimer D25 is composed of 24 units of phenylacetylenes, the γ_s per unit molecule (phenylacetylene) of D25 becomes 48 750 au, which is shown to be still about 2 times as large as that of diphenyacetylene (γ_s = 23 250 au). Judging from these results, we expect the π-electron conjugation length in the longitudinal direction (along the benzene-ring and acetylene units) of diphenylacetylene to significantly contribute to the enhancement of the component of γ. L25 is expected to have the largest π-conjugation length in the longitudinal direction because of the *para*-connection, while the π-conjugation length in D25 is predicted to be smaller than that in L25 because of the two-dimensional structure and the decoupling of π-conjugation at the *meta*-substitutions of benzene rings. To better elucidate the features of the contribution of electrons to γ, we next investigate the density distributions of the main components of γ for these compounds.

Figure 5a shows the γ_{zzzz} density distribution of L25, and Figures 5b and c shows γ_{xxxx} and γ_{zzzz} density distributions of D25, respectively. Apparently, for L25, the large γ density distributions are observed over the whole region of the chain. The magnitudes of these distributions are shown to be significantly larger than those of diphenylacetylene (Figure 4b). The both-end phenylacetylene regions (with a large distance) are found to provide a dominant positive contribution to the longitudinal γ of L25 although cancellation between positive and negative contributions is observed in the middle region of the chain. Such a large positive contribution of both-end regions

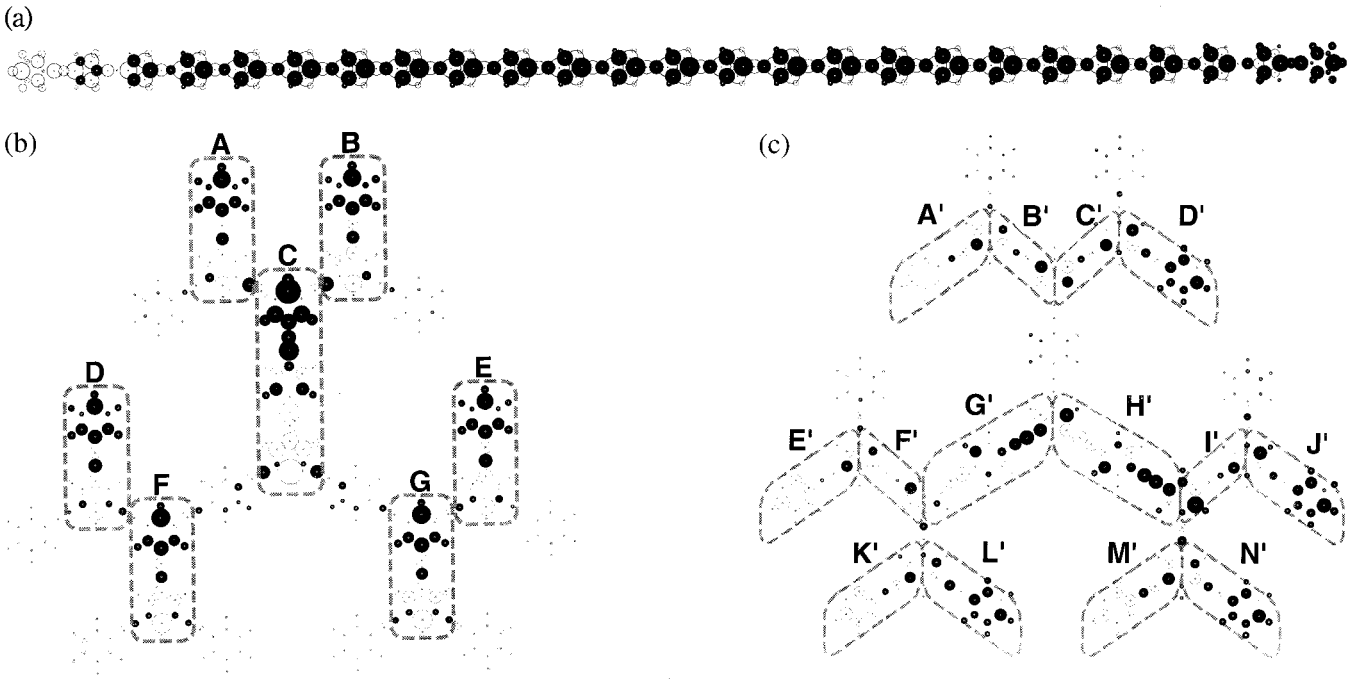

Figure 5. γ_{zzzz} (a) density plot of L25 (shown in Figure 1, compound **3**) and γ_{xxxx} (b) and γ_{zzzz} (c) density plots of D25 (Figure 1, compound **4**). These are calculated by the INDO/S CHF method. The white and black circles represent positive and negative γ densities, respectively, and the size of the circle indicates the magnitude of γ densities. The gray points indicate the positions of carbon atoms.

is ascribed to be the extension of π-conjugation in the chain-length direction. In contrast, the spatial contributions of γ_{xxxx} and γ_{zzzz} density distributions of D25 are found to be localized in the linear-leg regions, **A**−**G** for γ_{xxxx} and **A′**−**J′** for γ_{zzzz}, parallel to the directions, *x* and *z*, of the applied electric fields, respectively. For γ_{xxxx} density distributions (Figure 5b), all of the spatial contributions except for region **C** are found to be similar to those of diphenylacetylene (see Figure 4a), while the contribution (positive in sign) in the central linear-leg region **C** (composed of two phenylacetylene units) is found to be caused by the virtual excitation from one-side phenylacetylene to the other-side one, and its magnitude is shown to be more enhanced as compared to other contributions. These features suggest that π-conjugation is well localized in these linear-leg regions mutually connected by *meta*-substitutions and is enhanced in the central long *para*-connected linear-leg region **C** because larger π-conjugation decreases excitation energies and thus leads to the enhancement of the contribution to γ as expected by the perturbational formula of γ.[1−4] We here again consider the enhancement factor of γ_s/n of D25 with respect to that of diphenylacetylene (compound **1**). The complete suppression of π-conjugation at the *meta*-branching points is expected to cause the fact that the γ_s/n of D25 is similar to that of diphenylacetylene because only three parts of three-ring linear-leg regions (compound **2**) are involved, while others are diphenylacetylenes (compound **1**). However, as observed above, the γ_s/n of D25 (48750 au) is still about 2 times as large as that of diphenylacetylene (23250 au). This suggests that the slight π-conjugation via *meta*-branching points remains and thus further enhances the contribution to γ in linear-leg regions although this enhancement is much smaller than that of L25. To further investigate this feature, we consider the γ_{xxxx} density distributions of D25 (Figure 5b). Apparently, the dominant spatial contributions come from linear-leg regions **A**−**G** (Figure 5b). Therefore, we can estimate the approximate γ_{xxxx} per unit by considering these eight **A**−**G** regions ($\gamma_{xxxx}/8 = 271\,400$ au). If π-conjugation is completely suppressed at the *meta*-branching points, the γ_{xxxx} of D25 should be composed of the contributions from isolated **A**−**G** regions: one three-ling linear-leg molecule (501 400 au (see Figure 4b)) and six diphenylacetylenes ($6 \times$ 113 100 au (see Figure 4a)). The γ_{xxxx} per unit calculated from the group of the isolated linear-legs becomes 147 500 au, which is about one-half of $\gamma_{xxxx}/8 = 271\,400$ au in the case of the dendrimer. This implies that the contributions to γ_{xxxx} localized in linear-leg regions of D25 are totally about 2 times more enhanced than those of the group of isolated linear-leg regions. In fact, as shown in Figure 5b, the magnitudes of γ_{xxxx} densities in the central region **C** are somewhat more enhanced than those of compound **2** (Figure 4b) although the spatial contributions to γ_{xxxx} are well segmented and localized in each linear-leg region **A**−**G**. It is interesting that such enhancement is predicted to be caused by the slightly remaining π-conjugation via *meta*-branching points because, in general, π-conjugation suppression at the *meta*-branching points has been focused in relation to the unique functionality, for example, energy transfer from the periphery to the core, of these dendrimers.

On the other hand, for γ_{zzzz} density distributions (Figure 5c) in regions **K′**−**L′** and **M′**−**N′**, considerable cancellation of positive and negative contributions is observed at the *meta*-connected benzene rings, so that the primary contribution (positive in sign) seems to be caused by the virtual excitation from the one-end benzene ring to the other-end one. However, these features can be explained by the addition of the γ density distributions of diphenylacetylenes (see Figure 4a); γ density distributions on the central *meta*-connected benzene ring are similar to the sum of γ densities on the overlapped each end benzene ring of diphenylacetylenes arranged as shown in **K′**−**L′** and **M′**−**N′**, respectively. Such addition of γ density distributions of diphenylacetylenes and the nonenhancement of γ densities are predicted to reflect the well decoupling of the

π-conjugation at the *meta*-connected benzene rings. Similar features are also observed in regions **A′**−**B′**−**C′**−**D′**, **E′**−**F′**, and **I′**−**J′**. It is noted that the γ density distributions in regions **G′** and **H′**, which involve two units of phenylacetylenes, respectively, are more enhanced than those in other linear-leg regions and are also larger than those in isolated three-ring linear-leg regions (compound **2**, see Figure 4b), similar to the case of γ_{xxxx}. The contributions of electrons in these regions are shown to be positive in sign and to be caused by the virtual excitation from the one-side phenylacetylene unit to the other-side one, while the contributions are shown to be well segmented at the central *meta*-connected benzene ring. Similar to the γ_{xxxx} case, these features are predicted to relate to the well, but not complete, decoupling of π-conjugation at the central *meta*-connected benzene ring and to the structural feature that the π-conjugation length is larger in central linear-leg regions as compared to those in periphery regions.

In conclusion, the reason for the smaller γ_s value of D25 as compared to that of L25 is the smaller π-conjugation lengths in D25 (well-decoupled at the *meta*-connected benzene rings and localized in the linear-leg regions), the lengths of which are smaller than the chain length of L25. As expected from the γ density distributions of D25, however, the degree of increase in γ values and their spatial contributions on the two-dimensional plane of fractal antenna dendrimers can be controlled because the γ densities localized in linear-leg regions are considered to be building blocks (linear-legs) of γ values, which are still more enhanced than those of the same-size isolated linear-leg molecules because of slightly remaining π-conjugation via *meta*-branching points.

Conclusions

The present study elucidated that the contributions of electrons to γ for a phenylacetylene dendrimer (D25) with a fractal antenna structure are spatially localized although the hyperpolarizability has been considered to be a global quantity in general. The orientationally averaged γ value was found to be dominantly determined by the two components in the plane, γ_{xxxx} and γ_{zzzz}, which were shown to be contributed by the electrons in linear-leg regions parallel to the applied electric fields, *x* and *z*, respectively. It was further elucidated that such contributions are well segmented at the *meta*-connected benzene rings and are more enhanced in internal regions than those in outer (periphery) regions. These localizations of the spatial contributions of electrons to γ are presumed to originate in the fact that π-electron conjugation in linear-leg regions primarily contributes to the corresponding component of γ and is well decoupled at the *meta*-connected benzene rings, the feature of which can be easily understood by the absence of the resonance structure including the displacement of π-bonds via the *meta*-connected benzene ring. Such a feature of decoupling of π-conjugation, that is, the destruction of electronic coherency, at the *meta*-connected benzene rings is found to be in agreement with the previous results.[19] The enhancement of the contributions to γ in internal linear-leg regions can be primarily explained by the reduction of the excitation energies in the internal linear-leg regions because of the longer π-conjugation lengths as compared to the shorter π-conjugation lengths in outer regions. It is also noted that the magnitudes of the contributions to γ of such internal segments are more enhanced than those of the same-size isolated linear-leg molecules. This feature suggests that slightly remaining π-conjugation via *meta*-branching points still can contribute to the enhancement of γ in such segments involved in a dendrimer. From the comparison of γ of D25 with that of *para*-substituted phenylacetylene oligomers (L25), although the γ_s per unit molecule (diphenylacetylene) of D25 is shown to be about 2 times as large as that of diphenylacetylene, the γ_s value of D25 is found to be about 6 times as small as that of L25. This feature is found to originate in the smaller π-conjugation length of D25 than that of L25. Judging from these results, we expect the spatial contributions of electrons to γ for larger phenylacetylene dendrimers with fractal antenna structures to be localized in linear-leg regions and their contributions to increase on going from the periphery to the core. Such unique spatial contributions to γ reflect the fractal architecture of antenna dendrimers involving *meta*-connected benzene rings.

On the basis of the present study, we can predict the feature of γ of compact dendrimers (composed of all *meta*-connected same-length units) and the nonplanar effects on γ of dendrimers. From our previous studies on phenylene vinylene chains,[23] all *meta*-connected π-conjugated chains exhibit only slight enhancement of γ/n, which is similar to that of the unit molecule. Judging from the localization feature of γ density distributions in linear-leg regions shown in Figure 5b and c, we will observe similar features to all *meta*-connected chains in the full-size compact dendrimer case. Also, the actual extended dendrimers are expected to have somewhat nonplanar structures, in which linear legs may be bent at the *meta*-branching points. From the well-segmented γ density distributions (Figure 5b and c), the nonplanar structures are predicted to cause the further decrease in the π-conjugation via the *meta*-branching points. This will reduce the enhancement of γ/n observed in this study and cause the value to be closer to that of diphenylacetylene. Because the compact dendrimers more favorably take nonplanar structures than extended dendrimers because of their steric hindrance, the enhancement of γ/n because of π-conjugation via *meta*-branching points is predicted to be reduced, causing the γ/n of the compact dendrimer to be closer to the γ of the unit molecule.

One of the most important conclusions from this study is that quantum chemical calculations with our analysis methods using hyperpolarizability density can be used to understand the spatial contributions of electrons to γ. This result can directly elucidate the structure−property relation in γ. Another important conclusion is that the novel architecture of fractal antenna dendrimer involving *meta*-connected benzene rings closely relates to the unique feature of spatial contributions to γ. This result can then be employed to adjustably design novel molecular systems exhibiting desired NLO characteristics by constructing relevant fractal architecture composed of π-conjugation linear-legs and *meta*-connected benzene rings. Future publications will elucidate the structure−property relation in hyperpolarizabilities of related types of fractal dendrimers, for example, nanostar[15,47] and nonsymmetrical dendrimers,[48] and three-dimensional dendrimers,[5−14] as well as discussing the relation between energy transfer (exciton migration) and optical response properties.

Acknowledgment. This work was supported by Grant-in-Aid for Scientific Research (Nos. 14340184 and 14204061) from

(47) Kleiman, V. D.; Melinger, J. S.; McMorrow, D. *J. Phys. Chem. B* **2001**, *105*, 5595.
(48) Peng, Z.; Pan, Y.; Xu, B.; Zhang, J. *J. Am. Chem. Soc.* **2000**, *122*, 6619.

Japan Society for the Promotion of Science (JSPS) and a grant from the Ogasawara Foundation for the Promotion of Science & Engineering.

Supporting Information Available: The longitudinal component values, γ_{zzzz}, and their density plots of diphenylacetylene **1** (see Figure 1) calculated by the HF, MP2, B3LYP methods with 6-31G** and 6-31G**+d basis sets (Figure S1). The longitudinal component values, γ_{zzzz}, and their density plots of bis(phenylacetylene)-benzene **2** (see Figure 1) calculated by the HF, MP2, B3LYP methods with a 6-31G** (and 6-31G**+d for HF) basis set (Figure S2) (PDF). This material is available free of charge via the Internet at http://pubs.acs.org.

JA0115969